LAWRENCE
LIVERMORE
NATIONAL
LABORATORY

LLNL-JRNL-407763

Intense Pulsed Neutron Emission from a Compact Pyroelectric Driven Accelerator

V. Tang, G. Meyer, S. Falabella, G. Guethlein, S. Sampayan, P. Kerr, B. Rusnak, J. Morse

October 13, 2008

Journal of Applied Physics

Disclaimer

Intense Pulsed Neutron Emission from a Compact Pyroelectric Driven Accelerator

V. Tang, G. Meyer, S. Falabella, G. Guethlein, S. Sampayan, P. Kerr, and B. Rusnak, Lawrence Livermore National Laboratory, Livermore, CA 94551

J. D. Morse, National Nanomanufacturing Network, University of Massachusetts, Amherst, MA 01027

Abstract

Intense pulsed D-D neutron emission with rates $>10^{10}$ n/s during the pulse, pulse widths of ~100's ns, and neutron yields >10 k per pulse are demonstrated in a compact pyroelectric accelerator. The accelerator consists of a small pyroelectric $LiTaO_3$ crystal which provides the accelerating voltage and an independent compact spark plasma ion source. The crystal voltage versus temperature is characterized and compare well with theory. Results show neutron output per pulse that scales with voltage as $V^{\sim 1.7}$. These neutron yields match a simple model of the system at low voltages but are lower than predicted at higher voltages due to charge losses not accounted for in the model. Interpretation of the data against modeling provides understanding of the accelerator and in general pyroelectric $LiTaO_3$ crystals operated as charge limited negative high voltage targets. The findings overall serve as the proof-of-principle and basis for pyroelectric neutron generators that can be pulsed, giving peak neutron rates orders of magnitude greater than previous work, and notably increase the potential applications of pyroelectric based neutron generators.

I. Introduction

Simple and compact pyroelectric based accelerators [1-4] for neutron generation are of interest for various applications, including as a source for active interrogation of unknown threats containing explosives or nuclear materials [5]. For these applications, the ability to produce high intensity user-requested pulses of neutrons with very short pulse widths is highly desirable. Previous pyroelectric neutron sources produce neutrons in a continuous DC manner, relied on thermal cycling of the crystals for beam formation, and generally produced ion beams through sharp field ionizer tips coupled to positively charged crystals; this approach fundamentally has significant problems producing controllable pulses of neutrons with the timing typically desired for applications.

To achieve pulse operation in a proof-of-principle experiment, we have re-configured the LLNL CDNS experiment [4]. Specifically, by incorporating a compact independently controlled spark plasma ion source with a negative high voltage pyroelectric crystal, we are able to produce intense, user-controlled, pulsed D-D neutron emission with rates greater than ~10^{10} n/s during the pulse, pulse widths on the order of ~100's ns, and neutron yields greater than 10 k per pulse in the experiment. These peak neutron rates are orders of magnitude greater than previous work. The total neutron yield per thermal cycle is lower however than previous results using a conventional pyrofusion setup. Additionally, we have made systematic measurements of the crystal voltage against different thermal cycles. Here, we review the experimental setup and results, interpret the neutron and voltage measurements against theory to provide understanding of the accelerator and in general pyroelectric $LiTaO_3$ crystals operated at high negative voltages, and review methods to increase both the peak neutron rate and total neutron yield per thermal cycle.

II. Experimental setup and results

The current setup consists of a bare 3 cm diameter by 1 cm thick $LiTaO_3$ crystal coated with a ~6 μm thick deuterated polystyrene similar to the target crystal in ref [3] coupled to an independently operated spark plasma deuterium ion source [6-9]. The specific ion source used is discussed in depth in ref [8-9]. A schematic of the experiment is shown in Figure 1. The crystal surface is oriented for negative high voltage up to ~-100 kV when heated in 30 degree increments, and provides both the acceleration gradient and the deuterated target for D-D fusion. The rear of the crystal is grounded. The crystal is heated and cooled using a feedback controlled TE cooler as described in [4]. The spark ion source provides the ion beam for the accelerator and is operated with input pulse lengths of ~50 ns and voltages of ~4 kV, resulting in peak plasma spark currents of ~65 A shown in Figure 2. The D ions in the resultant plasma stem from deuterium liberated by the spark between the two strips of TiD_2 in the source. The ion beam is extracted through an aperture ~2 mm above the spark via electric fields from the crystal. Previous work at longer pulse lengths indicate that approximately less than half of the beam current is D^+, with the rest primarily made of various states of ionized Ti [6-7] and possibly D_2^+. The pulse width of the ion beam is not measured and could be greater than the applied current pulse length of 50 ns as the plasma can persist after the current pulse, possibly on the order of ~100's ns based on estimates of the plasma sound speed and the aperture gap. The pressure in the system is kept below 10^{-8} Torr. For diagnostics, a 14 tube ^{3}He array similar to the one in ref [4] is used; the total efficiency is $3(\pm 0.45) \times 10^{-3}$ detected neutrons per source neutron. For this study, the electronics render detected neutrons for a total 524 μs after they are triggered. The tubes are immune to x-rays and

electromagnetic noise from the pulser driving the ion source, and detect essentially zero (~0.001) background neutrons during the 524 μs of on-time. To diagnose the voltage remotely, a NaI gamma ray detector is available to measure bremsstrahlung endpoints from field emitted electrons. A CCD camera detects visible arcs or flashovers.

For the discussed experiments, a heating rate of 0.1 C^o/s was used with an initial starting temperature of 10 C^o. At this low heating rate, the crystal temperature is nearly even, with 1-D analytical solutions of the non-homogenous heat transfer PDEs indicating a differential of ~3 C^o between the rear and front of the crystal. An example run consists of a heating ramp from 10 C^o to 40 C^o, with the spark source being fired at 40 C^o; runs with higher endpoint temperatures allow the ion source to be fired more than once during the ramp. A cool down ramp follows which is completed with several firing of the spark source to neutralize any positive charges on the crystal; arcs or flashover breakdowns of the crystal also perform the same function. It is found that during optimal operation of the ion source, one firing of the ion source is sufficient to neutralize the crystal of either all or a significant portion of its build-up charge, as immediate subsequent firing of the source produces no detectable neutrons. Typically, the crystal is prone to flashovers or arcs after a temperature change of greater than 30 C^o giving voltages of ~-105 kV; firing the source after such an event also results in no detectable neutrons. In addition, visible flashovers over the crystal surface are common when the ion source is fired onto a negative voltage crystal, especially in the ~-100 kV range. This suggests breakdowns caused by secondary electrons from the impinging ion beam.

Concerning the bremsstrahlung spectra and crystal voltages, in addition to data from neutron experiments, runs with the spark source replaced by a thin tungsten foil to increase bremsstrahlung signal and with the NaI detector at various angles to the foil were performed to deduce voltages for different temperature cycles. From a theoretical point of view, neglecting complicated field emission losses, the crystal voltages can be estimated via:

$$C_{cr}\frac{dV}{dT} = K_p(T)A - \frac{V(T)}{\gamma R(T)} \quad (1)$$

Where V is the surface voltage of the crystal, C_{cr} is its capacitance, calculated via 2-D electrostatic simulation and estimated as ~30 pF, T the temperature, K_p the pyroelectric coefficient, from 170 to 190 $\mu C/m^2C^o$ in the temperature range of interest [10-11], A is the area of the crystal and is 7.1 cm^2, γ the heating rate in C^o/s, and R is the crystal resistance as a function of temperature [12]. The bulk resistance of the crystal spans ~130 TΩ to 17 TΩ from 10 C^o to 80 C^o.

Figure 3 plots the calculated voltage against temperature for a 0.1 C^o/s ramp using Equation 1 with data from bremsstrahlung endpoints. A sample spectrum indicating a crystal voltage of ~-95 kV is shown in the insert. The data agrees with the model quite well, with a ~10% difference near the 100 kV region where field emission current from the crystal plays a larger role in the crystal charge balance. Experimentally, notably greater bremsstrahlung flux for these higher voltages is observed, as expected.

Figure 4 plots the neutron yield per pulse as a function of voltage for three run series performed sequentially. The voltages are determined using Equation 1, with the 10% reduction taken into account for voltages at ~-100 kV. The experiment can thus deliver approximately 2 pulses of more than 10 k neutrons for a temperature ramp from 10 C^o to 80 C^o, with rates easily exceeding 10^{10} n/s during optimum operation as shown in the first and third series. The second series clearly produced fewer neutrons which might be due to local depletion or damage of the deuterated strip in the ion source where the arc was repeatedly situated. In fact, for these runs, neutrons were detected when the source was fired for a second time at a particular temperature, indicating significantly lower beam currents compared with optimum source operation. The third series show recovered yields and again optimum operation; it is theorized that for this series the arc on the ion source moved to a different region of the deuterated strip. A power fit of the first series, with admittedly large scatter, gives a scaling of $Y \sim V^{1.7}$ neglecting the two very low yield points near -100 kV. The two anomalous low yields could be due to the crystal having voltages lower than indicated when the source fired. A flashover might have occurred before the firing that was not captured by the CCD camera. Another possibility is again local depletion or damage on the arc source since one of the low yield points is from the last run in the first series.

III. Analysis and Methods to Further Increase Yields

Although the peak neutron rates in our current experiment are orders of magnitude higher than in comparison with previous experiments, the total neutron yield per comparable thermal cycle is lower, around 20% of ref [1, 4]. We suspect this is caused by several factors; (1) parasitic Ti^{1-3+} from the ion source, (2) loss of charge from ejected secondary electrons on the crystal surface due to the impinging ion beam and any resultant flashovers, and (3) less effective use of the crystal charge due to the essentially instantaneous high current ion beams extracted from the spark source. On (1), less than half [6] of the spark source ion beam is D^+, the rest being parasitic ions and charge

neutralizers that do not produce neutrons. In contrast, as in ref [4], the conventional pyrofusion setup can produce almost pure D^+ beams. On (2), flashovers are commonly seen when the ion source is fired as discussed. Concerning (3), the extracted ion beam from the spark source is large enough to neutralize all or nearly all of the charge on a ~-100 kV crystal. This means that portions of the beam current during the pulse are effectively at lower energies, resulting in a lower cross-section for D-D reactions. Because of the very short pulse lengths of these ion beams the crystal cannot maintain a steady high voltage through the pyroelectric effect during the beam pulse as in a conventional pyrofusion experiment. A simple model of the system yield which includes most of these factors follows. Assuming the ion source provides enough charge to neutralize the crystal completely when fired, the total neutron yield per pulse at a specific crystal voltage can be estimated via:

$$Y(V) = L_s f_D \int_0^V n(V) C_{cr} dV \quad (2)$$

Where n(V) is the calculated yield per Coulomb of D^+ ion with energy eV onto a thick fully deuterated polystyrene target using stopping powers from SRIM [13] and D-D neutron branch cross sections from ref [14], f_D is the fraction of ion current that is D^+ and assumed to be 0.5, and L_s are charge losses from secondary electrons and taken as 0.5 which corresponds to one ejected electron per ion. The model give a yield scaling of $Y \sim V^4$, and is plotted against the data in Figure 4. The measured yields in Figure 4 match the prediction at lower voltages but are lower than predicted at higher voltages probably due to the flashovers discussed in factor (2) which are unaccounted for in the model. We are working on more systematic studies of the total crystal charge losses due to the ion beam to resolve this discrepancy. In addition we are creating more detailed coupled models of the spark source with the crystal in order to determine the beam current extracted from the source and the neutron yield self-consistently for comparison with experiment.

Several methods are available empirically to increase the total neutron yield and intensity further based on the understanding above. A deuterated polyethylene coating can be used immediately which doubles the deuterium loading per carbon and thus doubles the neutron yield. On the ion source side, we are reviewing methods to gate the source in order to reduce parasitic ions and maximize the D^+ fraction in addition to finding the optimum ion source voltage, current, and rep rate. Suppression of secondary electrons from the crystal would mitigate charge losses. Lastly, we are examining ways to increase the crystal voltage which can increase the yield significantly.

IV. Conclusion

By coupling a user-controlled ampere class spark deuterium ion source with a negative high voltage pyroelectric crystal, we have demonstrated a pyroelectric neutron source with pulse output and peak neutron rates orders of magnitude greater than previous work. Interpretation of the results using simple models provides understanding of the accelerator and negative high voltage sources based on pyroelectric crystals. The ability now to produce user-controlled high intensity pulses of neutrons maximizes the potential applications of compact pyroelectric based neutron generators.

V. Acknowledgment

We thank Steve Letts for providing the deuterated polystyrene and for developing the coating process, Ed Cook for the use of his fast pulser which drove the ion source, and Elaine Hart for formulations of the crystal properties versus temperature. This work was supported by the Defense Advanced Research Projects Agency under contract 1026419 and the LLNL Laboratory Directed Research and Development program with the auspices of the U.S. Department of Energy by Lawrence Livermore National Laboratory under contract DE-AC52-07NA27344.

References

[1] B. Naranjo, J. K. Gimzewski, and S. Putterman, Nature, 434, 1115 (2005).

[2] J. Geuther and Y. Danon, J. Appl. Phys., 97, 074109 (2005).

[3] J. Geuther, Y. Danon, and F. Saglime, Phys. Rev Letts. 96, 054803-1 (2006).

[4] V. Tang, G. Meyer, J. Morse et al., Rev. Sci. Inst., 78, 123504 (2007).

[5] V. Tang, G. Meyer, S. Falabella et al., AIP Proceedings, 20th International Conference on the Application of Accelerators in Research and Industry (2008). (In press)

[6] E. Cheifetz, U. Adar, and G. Davara, Proc. XVIIth International Symposium on Discharges and Electrical Insulation in Vacuum-Berkeley, (1996).

[7] A. A. Vasiliev, D. D. Iosseliani, V. V. Kushin et al., Problems of Atomic Science and Technology, 1 (2004).

[8] S. Falabella, G. Guethlein, P. L. Kerr et al., AIP Proceedings, 20th International Conference on the Application of Accelerators in Research and Industry (2008). (In press)

[9] G. Guethlein, S. Falabella, S. E. Sampayan et al., ibid

[10] M. E. Lines and A. M. Glass, Phys. Rev. Lett. **39**, 1362 (1977).

[11] A. M. Glass, Phys. Rev. **172**, 564 (1968).

[12] S. Leng and Y. Yu, Physica status solidi. A. Applied research, **143**, 431 (1994).

[13] J. F. Ziegler, J. P. Biersack, and U. Littmark, The Stopping and Range of Ions in Matter (Pergamon, New York, 2003).

[14] B. H. Duane, Fusion Cross Section Theory, Rept. BNWL-1685 (Brookhaven National Laboratory, 1972).

Figure Captions:

Figure 1: Schematic of the experiment.

Figure 2: Typical spark ion source current profile.

Figure 3: Bremsstrahlung deduced crystal voltages and predicted voltages based on Equation 1. The insert shows a sample bremsstrahlung spectrum indicating a crystal voltage of ~-95 kV.

Figure 4: Measured neutron yields and rates as a function of voltage for three run series. A power fit of $Y=0.015V^{1.7}$ is shown for the first series. The error bars are not shown on the 2nd and 3rd series for clarity. The neutron rate is calculated assuming a conservative long 1 μs pulse width. The model curve gives predicted yields using Equation 2 which scales as $\sim V^4$; at -100 kV, the detected yields are ~2 times lower than given by the simple model.

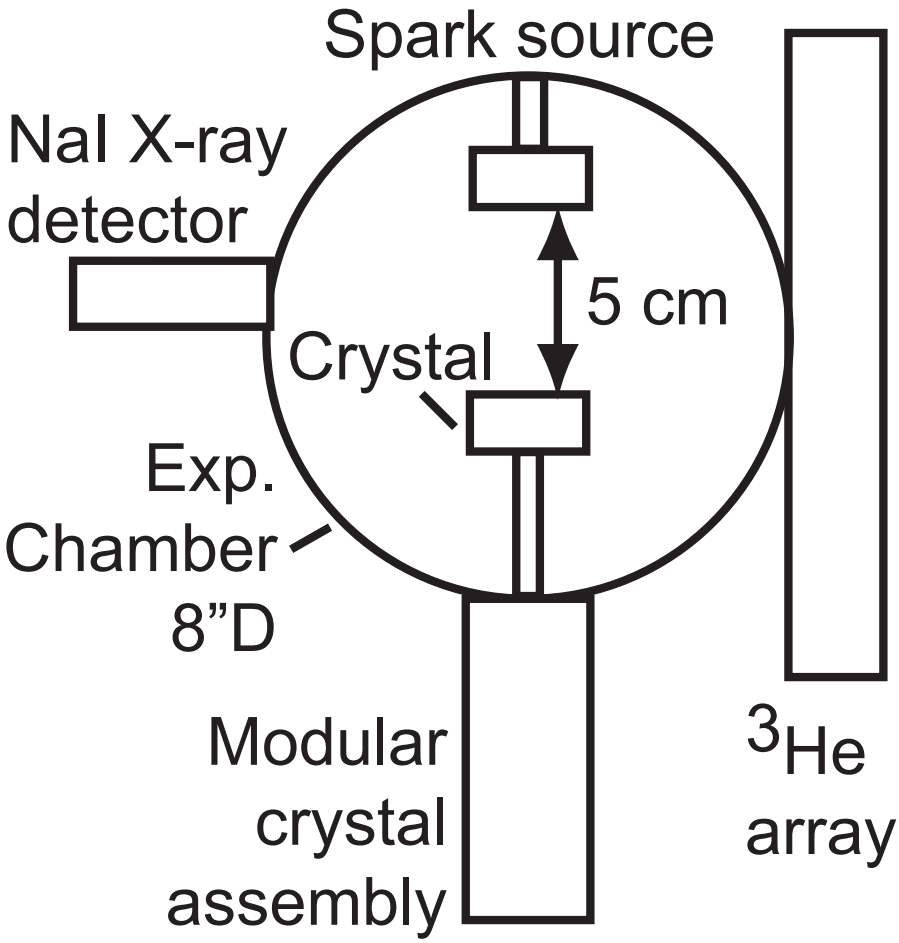
Spark source
NaI X-ray
detector
5 cm
Crystal
Exp.
Chamber
8”D
Modular
crystal
assembly
^{3}He
array

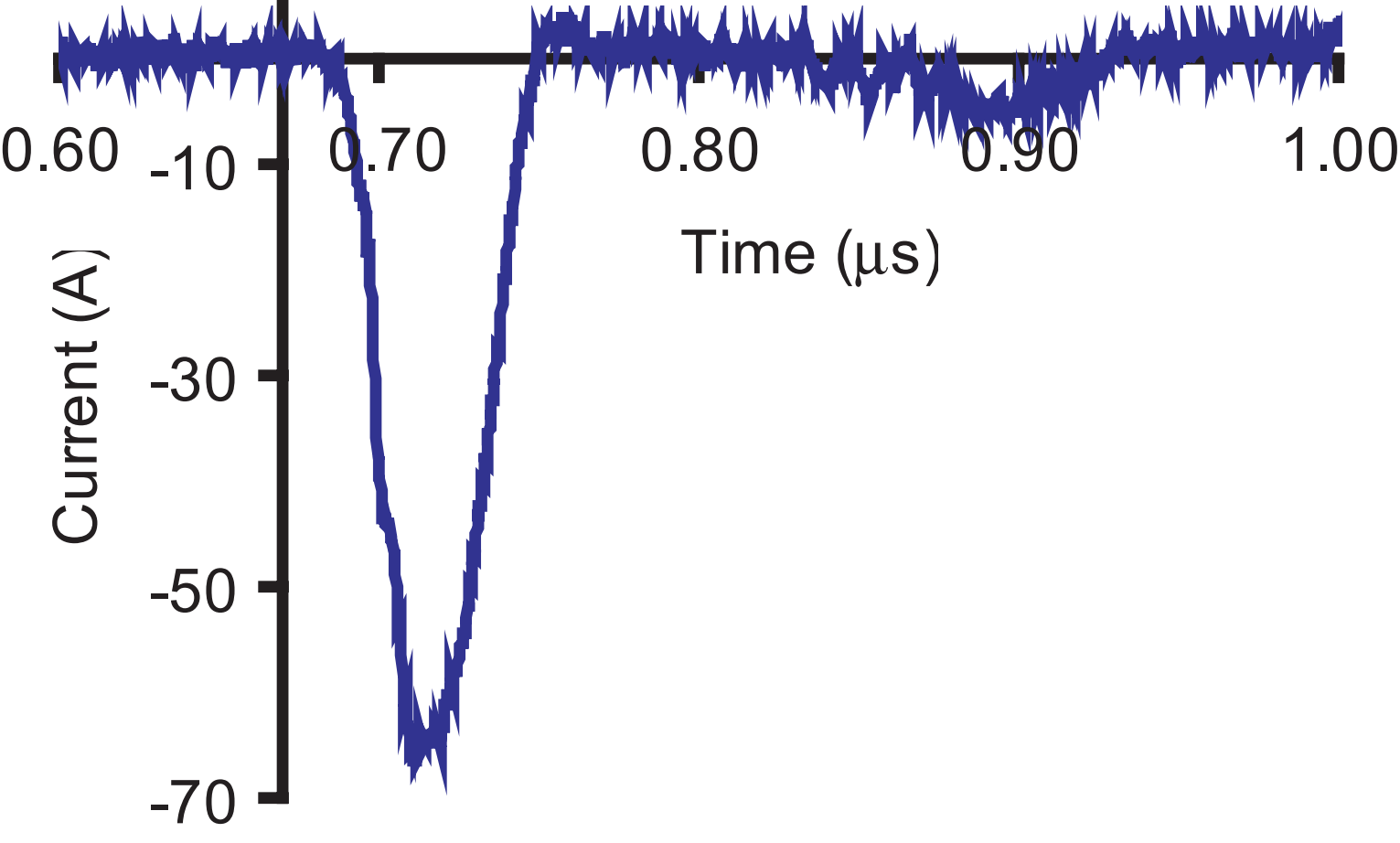
0.60
0.70
0.80
0.90
1.00
Time (µs)
-10
-30
-50
-70
Current (A)

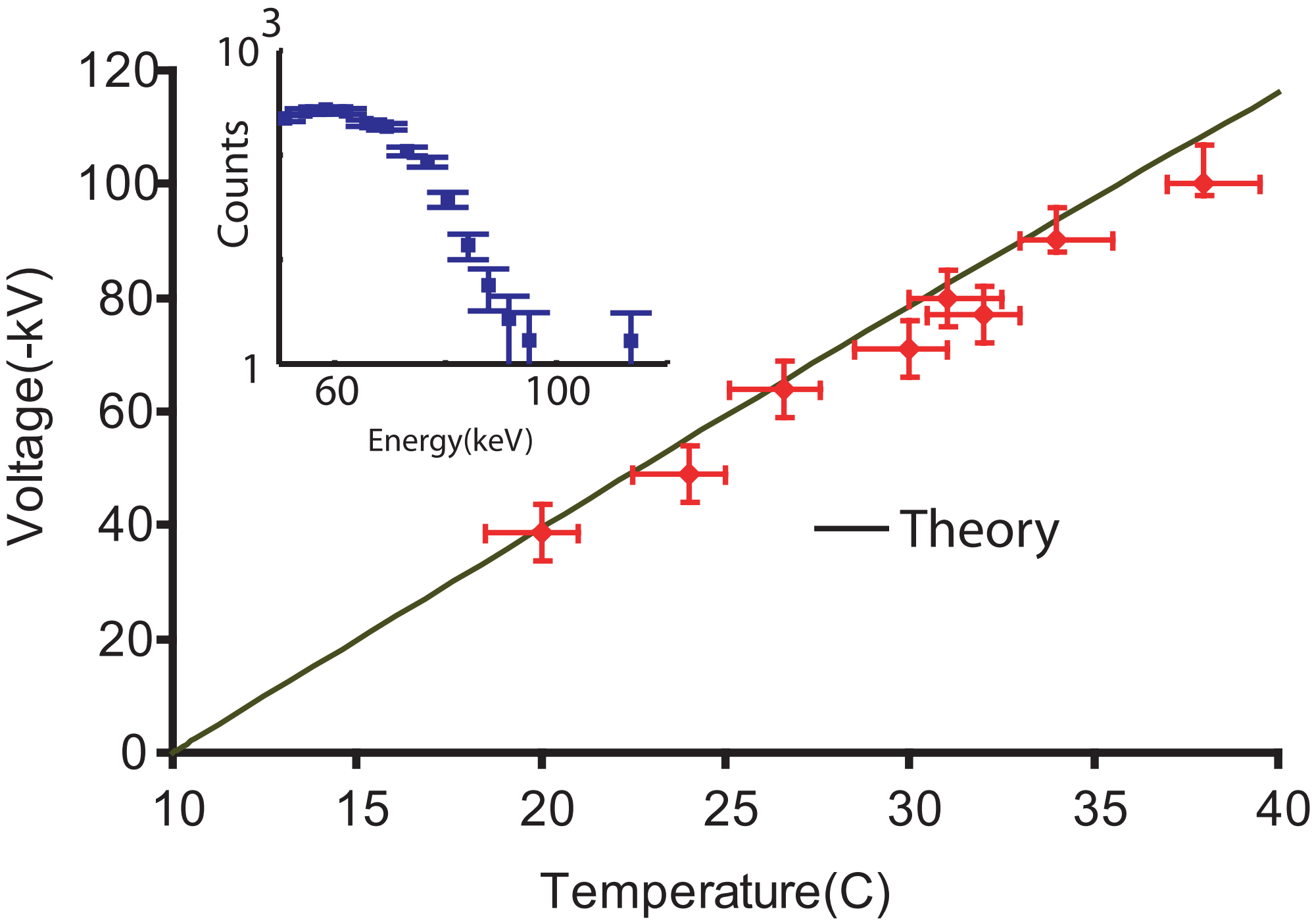
Voltage(-kV)
120
100
80
60
40
20
0
10
15
20
25
30
35
40
Temperature(C)
Theory
Counts
10^3
1
60
100
Energy(keV)

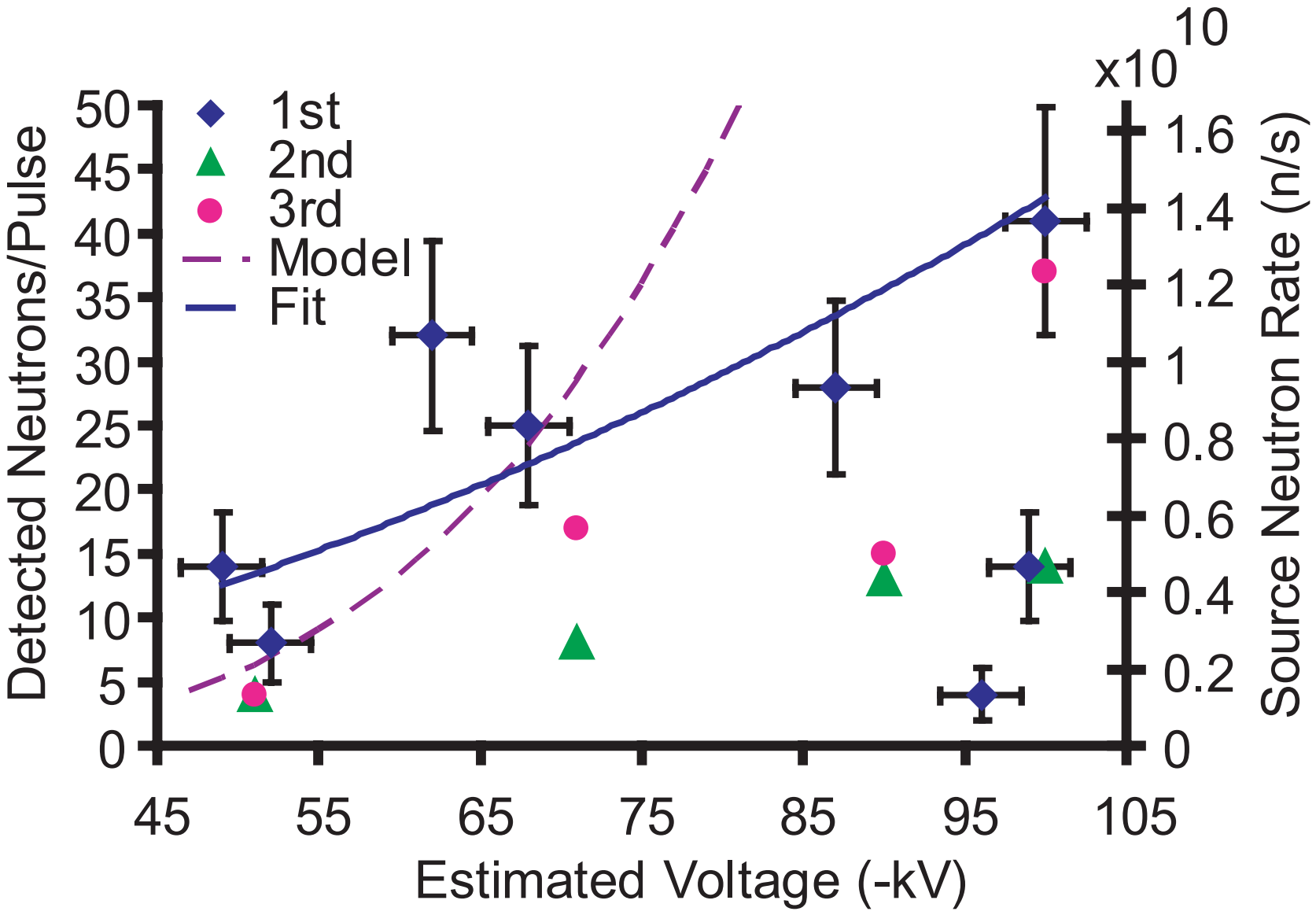
1st
2nd
3rd
Model
Fit
Detected Neutrons/Pulse
Source Neutron Rate (n/s)
x10^10
Estimated Voltage (-kV)
0
5
10
15
20
25
30
35
40
45
50
0
0.2
0.4
0.6
0.8
1
1.2
1.4
1.6
45
55
65
75
85
95
105